© 2017. Published by The Company of Biologists Ltd | Development (2017) 144, 866-875 doi:10.1242/dev.140368

RESEARCH ARTICLE

The E3 ubiquitin ligase Nedd4/Nedd4L is directly regulated by microRNA 1

Jun-yi Zhu[1], Amy Heidersbach[2,3], Irfan S. Kathiriya[2,4], Bayardo I. Garay[2,4], Kathryn N. Ivey[2,3], Deepak Srivastava[2,3], Zhe Han[1,*] and Isabelle N. King[2,3,*]

ABSTRACT

miR-1 is a small noncoding RNA molecule that modulates gene expression in heart and skeletal muscle. Loss of *Drosophila miR-1* produces defects in somatic muscle and embryonic heart development, which have been partly attributed to *miR-1* directly targeting Delta to decrease Notch signaling. Here, we show that overexpression of *miR-1* in the fly wing can paradoxically increase Notch activity independently of its effects on Delta. Analyses of potential *miR-1* targets revealed that *miR-1* directly regulates the 3′UTR of the E3 ubiquitin ligase *Nedd4*. Analysis of embryonic and adult fly heart revealed that the Nedd4 protein regulates heart development in *Drosophila*. Larval fly hearts overexpressing *miR-1* have profound defects in actin filament organization that are partially rescued by concurrent overexpression of Nedd4. These results indicate that *miR-1* and Nedd4 act together in the formation and actin-dependent patterning of the fly heart. Importantly, we have found that the biochemical and genetic relationship between *miR-1* and the mammalian ortholog Nedd4-like (*Nedd4l*) is evolutionarily conserved in the mammalian heart, potentially indicating a role for Nedd4L in mammalian postnatal maturation. Thus, *miR-1*-mediated regulation of Nedd4/Nedd4L expression may serve to broadly modulate the trafficking or degradation of Nedd4/Nedd4L substrates in the heart.

KEY WORDS: miR-1, Nedd4, Nedd4L, Nedd4-2, Heart

INTRODUCTION

Notch signaling regulates many aspects of cell differentiation and specification. In the developing *Drosophila* wing, Notch cooperates with the Hedgehog (Hh) pathway to form and pattern the anterior-posterior (AP) boundary (Casso et al., 2011). Several E3 ubiquitin ligases assure that Notch and its ligands properly migrate from the cell surface to various endocytic compartments for activation (e.g. Deltex, Mindbomb1). By contrast, the E3 ubiquitin ligase Nedd4 (neural precursor cell-expressed, developmentally downregulated 4) negatively regulates Notch by directing it to the lysosome (Ingham et al., 2004; reviewed by Rotin et al., 2000; Sakata et al., 2004). Nedd4, along with its family of proteins, has a phospholipid-binding C2 domain, two to four WW domains that recognize substrates, and a catalytic domain homologous to the E6-AP C-terminal (HECT) domain (reviewed by Rotin and Kumar, 2009). Although its regulation is relatively unexplored, Nedd4 activity is governed by multiple post-translational modifications and an array of co-factors (reviewed by Yang and Kumar, 2010).

MicroRNA 1 (*miR-1*) is evolutionarily conserved from flies to humans and is crucial for normal cardiac development and function (Heidersbach et al., 2013; Ivey et al., 2008; King et al., 2011; Kwon et al., 2005; Sokol and Ambros, 2005; Wei et al., 2014). *Drosophila miR-1* negatively regulates the Notch ligand Delta in the developing *Drosophila* wing, producing a loss of Notch activity (Kwon et al., 2005). Using a *GAL4-UAS*-based system in the fly wing, we identified genetic pathways that intersect with *miR-1* (King et al., 2011). This system is particularly adept at detecting interactions between *miR-1* and the Notch pathway due to the importance of Notch signaling in wing-vein patterning. Specifically, increased Notch signaling results in a loss of vein structures, whereas decreased Notch signaling results in thickened, tortuous veins (de Celis and García-Bellido, 1994). Unexpectedly, we observed a progressive loss of vein structures as *miR-1* levels rose, suggesting that, in certain contexts, *miR-1* can promote Notch signaling. Given this unexpected result, we speculated that in addition to its effects on Delta, *miR-1* also governs the activity of a negative regulator (or regulators) of the Notch pathway. To identity this *miR-1* target, we focused on a particular vein phenotype that results in a truncated third long vein (L3).

RESULTS

Overexpression of *miR-1* in the wing can increase Notch signaling

Using the *decapentaplegic*-GAL4 driver (*dpp-GAL4*) system, we expressed *Drosophila miR-1* specifically in the AP organizer of the wing imaginal disc (*dpp>miR-1*) (Brand and Perrimon, 1993; King et al., 2011). Capitalizing on the temperature responsiveness of the *GAL4-UAS* system, we placed the *dpp>miR-1* line at 20°C or 22°C and scored the wings for changes in vein patterning and L3/L4-intervein distance. As *miR-1* expression increased, the wing veins thickened and intervein distance decreased progressively, consistent with *miR-1* repressing the Notch ligand Delta in the AP organizer. Unexpectedly, at 22°C, when *miR-1* expression is highest, a significant number of flies were missing the distal region of L3, a wing phenotype similar to that produced by increased Notch signaling (Fig. 1A, lower panel; Fig. 1B).

Next, we focused on the molecular mechanism of this truncation. To determine whether the distal loss of L3 under conditions of high *miR-1* expression reflected increased Notch signaling, we genetically crossed alleles of positive and negative regulators of the Notch pathway. All parental lines had wild-type L3-vein morphology (data not shown). When mated to *dpp>miR-1* flies, fly lines containing loss-of-function alleles of positive regulators of Notch (i.e. *Notch*, *deltex*, *Suppresssor of Hairless*) showed a variable loss of intervein distance, indicating a genetic interaction with *miR-1* (Fig. S1A).

[1]Children's National Medical Center, Washington, DC 20010, USA. [2]Gladstone Institute of Cardiovascular Disease, San Francisco, CA 94158, USA. [3]Department of Pediatrics, University of California, San Francisco, CA 94143, USA. [4]Department of Anesthesia and Perioperative Care, University of California, San Francisco, CA 94143, USA.

*Authors for correspondence (zhan@childrensnational.org; isabelle.king@gladstone.ucsf.edu)

J.Z., 0000-0002-4517-101X; D.S., 0000-0002-3480-5953; Z.H., 0000-0002-5177-7798; I.N.K., 0000-0002-3182-7540

Received 1 June 2016; Accepted 10 January 2017

Development (2017) 144, 866-875 doi:10.1242/dev.140368

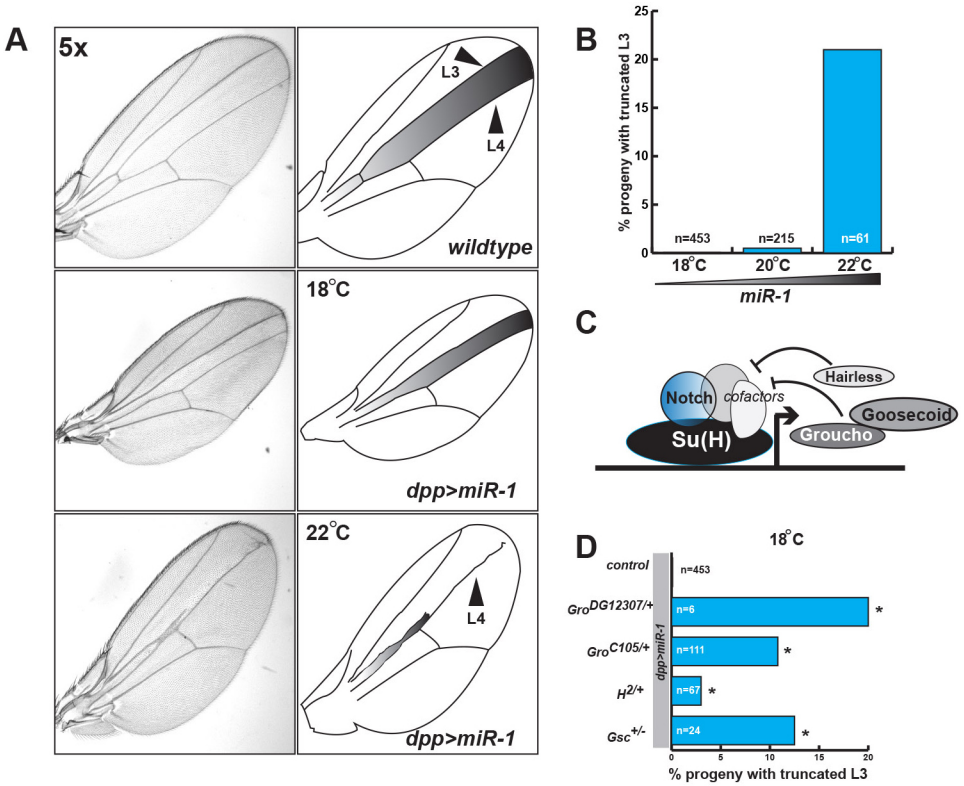

Fig. 1. Misexpression of *miR-1* in the anterior-posterior organizer causes a derepression of the Notch pathway. (A) Representative wings (left) and schematic of wing phenotypes are shown (right). Shaded areas indicate regions of *dpp-GAL4* activity, such that *miR-1* is overexpressed in the *dpp>miR-1* fly line. (B) Quantification of *dpp>miR-1* progeny lacking the distal region of L3 at different temperatures. The *UAS-GAL4* system allows titration of expression by temperature manipulation. *n*, number of progeny scored. (C) A simplified schematic of Notch repression. In the nucleus, Notch associates with its DNA-binding partner Suppressor of Hairless [Su(H)] to activate downstream target genes, some of which repress Notch signaling in a negative-feedback loop. (D) Percentage of progeny with a truncated L3 by genotype when crossed with the *dpp>miR-1* line at 18°C. At this temperature, L3 forms normally in the control *dpp>miR-1* line and loss of the L3-L4 intervein distance predominates. *n*, number of progeny scored. **P*<0.001. Gro, Groucho; Gsc, Goosecoid; H, hairless.

However, none of these alleles generated flies that lacked the distal region of L3, suggesting that reductions in the gene dose of Notch effectors were not responsible for the shortening of L3.

Dysregulation of Delta ubiquitylation or expression does not reduce L3 length

To determine whether dysregulation of Delta caused the loss of L3 structures, we manipulated the relative amounts of active Delta with mutants of *mindbomb1* (*mib1*) and UAS lines expressing wild-type or dominant-negative *Delta* (*UAS-Delta and UAS-Delta*$^{D/N}$, respectively). Mib1 facilitates the activation of Delta through ubiquitylation and subsequent endocytosis of the ligand (Itoh et al., 2003). Interestingly, reduced levels of *mib1* did not affect the *dpp>miR-1* phenotype, suggesting that the loss of L3 is not sensitive to the level of Mib1 expression in this system (Fig. S1B). Likewise, when crossed with the *dpp>miR-1* line, neither the *UAS-Delta* nor the *UAS-Delta*$^{D/N}$ lines produced offspring with L3 truncation (Fig. S1B). Wings overexpressing both *miR-1* and *Delta*$^{D/N}$ had a thickened and tortuous L3; however, the most distal region of L3 could not be reliably visualized, as the wings were globally deformed (data not shown). These results suggest that *miR-1*-mediated reduction of Delta or gross perturbation of Delta expression is insufficient to inhibit L3 formation.

Reductions in the dose of Notch co-repressors lead to L3 truncation

The Notch receptor associates with its DNA-binding partner Suppressor of Hairless [Su(H)] to activate several downstream genes, some of which form a negative-feedback loop (Fig. 1C). When we crossed transgenic lines containing loss-of-function alleles of Notch co-repressors (i.e. *groucho*, *hairless* or *goosecoid*) with the *dpp>miR-1* line, we observed an enhanced loss of intervein distance and a truncated L3 – phenocopying the wings of *dpp>miR-1* flies raised at 22°C (Fig. 1D). These results were obtained at 18°C, where *miR-1* expression is below the usual threshold for suppression of L3 formation. From these results, we concluded that the distal loss of L3 results from de-repression of the Notch pathway and reflects an epistatic relationship between *miR-1* and Notch repressors.

Truncation of L3 in *dpp>miR-1* flies is not due to phosphorylation of Groucho by receptor tyrosine kinases

Loss-of-function alleles of *groucho*, *hairless* or *goosecoid* could impair L3 formation by genetically interacting with a separate genetic pathway that is also required for vein formation in the wing. For example, epidermal growth factor receptor (EGFR) signaling modulates Notch activity through phosphorylation of Groucho mediated by tyrosine receptor kinase (Hasson et al., 2005). To determine whether the length of L3 is sensitive to EGFR activity, we tested effectors of EGFR signaling, both positive [e.g. Spitz (*spi*), Star (*S*), Rhomboid (*Rho*), Vein (*vn*) and Roughoid (*ru*)] and negative [e.g. Knot (also known as Collier) (*kn*), Argos (*aos*)]. Isolated alleles of *S*, *Rho*, *ru*, *spi*, *vn*, *aos*, or *kn* were crossed with the *dpp>miR-1* line. Scoring of the genetically relevant progeny did not reveal a genetic interaction between the EGFR pathway and *miR-1* (Fig. S2). However, their interaction was genetically enhanced when fly lines were deficient in *ED207* and *BSC289*. These lines are haploinsufficient at both the *Rho* and *ru* loci, and produce a variation in the intervein distance between L3 and L4 (the fourth long vein). However, in no instance did a reduction in gene dose of positive or negative regulators of EGFR signaling cause loss of the distal region of L3, nor did alleles of constitutively active EGFR (*Elp*^{B1}/*ellipse*) affect L3 formation (Baker and Rubin, 1989) (Fig. S2). Thus, L3 shortening does not depend on EGFR signaling or EGFR-mediated phosphorylation of Groucho.

miR-1 regulates the Notch pathway through conserved targeting of Nedd4

To explore the possibility that *miR-1* directly downregulates *groucho*, *hairless* or *goosecoid*, we interrogated the Targetscan

Development (2017) 144, 866-875 doi:10.1242/dev.140368

fly database (www.targetscan.org) and determined that no probable *miR-1* sites exist in the 3′UTRs of these genes. By contrast, *Su(H)*, *mib1* and *Nedd4* each contain one evolutionarily conserved *miR-1* site (data not shown). Interestingly, in *Drosophila* Schneider 2 (S2) cells transiently transfected with *miR-1*, followed by immunoprecipitation of Argonaut1 (Ago1) and quantitative RT-PCR, *Nedd4* mRNA was enriched (Easow et al., 2007). These results support the hypothesis that *miR-1* and *Nedd4* mRNA physically associate with each other within a miRNA-effector complex. These findings prompted us to focus on a possible genetic or biochemical relationship between *miR-1* and *Nedd4*.

Nedd4 ubiquitylates the PPSY motif in the intracellular domain of Notch in a HECT domain-dependent fashion (Sakata et al., 2004). Ubiquitylation of this motif by Nedd4 or Suppressor of Deltex [Su(dx)] reduces Notch signaling by directing the receptor to late endosomes. Nedd4-like proteins are evolutionarily conserved from yeast to mammals. *Nedd4* and its murine orthologue Nedd4L (also known as Nedd4-2) share a common domain structure (Fig. 2A). Nedd4 localizes to the cell membrane through its C2 domain and uses its WW domains to recognize substrate proteins. It negatively regulates Notch signaling by directing the Notch receptor towards endocytosis and lysosomal degradation. Interestingly, the predicted *miR-1* binding site in the 3′UTR of *Nedd4* and *Nedd4l* is widely conserved (Fig. 2B).

We hypothesized that the loss of L3 structures is due to *miR-1*-mediated downregulation of *Nedd4*. To test this hypothesis, we analyzed alleles of *Nedd4* in the wing assay at both 18°C and 20°C. At 18°C, the *dpp>miR-1* line had minimal *miR-1* expression, and penetrance of the L3 truncation phenotype was low but measurable with two *Nedd4* alleles ($Nedd4^{MI07766}$, 4.7%, n=103; $Nedd4^{C153}$, 2.3%, n=130; data not shown). At 20°C, where truncation of L3 is detected in the *dpp>miR-1* line, all alleles of *Nedd4* generated significant numbers of progeny with a shortened L3 (Fig. 2C, Fig. S3). The weakest allele, $Nedd4^{T119FS}$, also generated progeny with L3 breaks (17%, n=54; data not shown). Thus, reducing the *Nedd4* dose enhances the effects of *miR-1*, resulting in loss of L3 structures. To verify that the loss of Nedd4 activity was responsible for the effects on L3 formation, flies harboring a wild-type *Nedd4* construct (*UAS-Myc-Nedd4*) (Myat et al., 2002) were crossed to the *dpp>miR-1* line. For all alleles tested, concurrent overexpression of wild-type Nedd4 robustly reduced the number of progeny lacking the distal region of L3 (Fig. 2D). To determine whether an intact HECT domain was necessary for rescue of the wing vein phenotype, we crossed a line containing a ubiquitin ligase inactive Nedd4 construct [*UAS-Myc-Nedd4(C/A)*] with the *dpp>miR-1* line (Myat et al., 2002). Again, we observed marked suppression of the wing vein phenotype for all alleles except for $Nedd4^{T119FS}$ and $Nedd4^{C153}$ (Fig. 2E). These results suggest that the L3 truncation is attributable to reduced levels of Nedd4, though an intact HECT domain is not essential for this effect.

The genetic interaction between *miR-1* and *Nedd4* does not extend to other closely related E3 ubiquitin ligases

Like Nedd4, Su(dx) negatively regulates Notch. In wing discs, *Nedd4* can compensate for the loss of Su(dx), implying functional redundancy (Wilkin et al., 2004). Therefore, we sought to determine whether *miR-1* interacts genetically with other members of the *Nedd4* family [i.e. Su(dx), Smurf] using L3 morphology as a readout. $Su(dx)^{32}$, but not $Su(dx)^{KG02902}$ or $Su(dx)^{2}$, generated flies with a shortened L3. Similarly, $Smurf^{KG07014}$, but not $Smurf^{MI07104}$ or $Smurf^{s\text{-}160}$, genetically interacted with *miR-1* to repress L3 formation (Fig. 2F). These results indicate that L3 shortening cannot be generalized beyond the interaction of *miR-1* and *Nedd4* and that Nedd4 family members have non-redundant functions in our *dpp>miR-1*-based system.

Reduced Nedd4 activity is due to a functional *miR-1*-binding site in the 3′UTR of *Nedd4*

The 3′UTRs of fly *Nedd4* and murine *Nedd4l* are bioinformatically predicted to contain *miR-1*-binding sites (Fig. 2B). To assess the biological relevance of these putative sites, we cloned the 3′UTRs of *Nedd4 or Nedd4l* into luciferase-reporter constructs. Introduction of the *miR-1* mimic into the murine C2C12 myoblast cell line significantly reduced luciferase activity, suggesting that *miR-1* negatively regulates *Nedd4* mRNA in mammalian cells (Fig. 2G, left). Deletion of the putative *miR-1* seed sequence within the predicted target site prevented the repressive effects, demonstrating that silencing is *miR-1* dependent (Fig. 2G, right). Parallel studies also performed in the C2C12 myoblast cell line using the *Nedd4l* 3′ UTR produced similar results (see Fig. 6A), suggesting that the regulation of *Nedd4* and *Nedd4l* by *miR-1* is evolutionarily conserved.

Nedd4-null flies have abnormal heart specification and patterning that result in early lethality

To determine whether the genetic and biochemical relationship between *miR-1* and *Nedd4* was relevant in tissues where *miR-1* is endogenously expressed, we examined the cardiac phenotypes of the two *Nedd4* mutant alleles ($Nedd4^{T119FS}$ and $Nedd4^{MI07766}$) in a *Hand-GFP* (Han and Olson, 2005) background, which supports visualization of cardioblasts and pericardial cells in the developing fly heart. Analysis of these animals revealed that *Nedd4* is necessary for normal heart formation in the embryonic period and first instar stage (Fig. 3). Homozygous null *Nedd4* embryos were distinguished using a GFP-positive balancer chromosome and stained with antibodies against Mef2, a marker of somatic and heart muscle. We observed that most homozygous *Nedd4* mutants displayed reduced numbers of cardioblasts and pericardial cells at stage 15, resulting in gaps among the two rows of cardioblasts (Fig. 3A-C). Homozygous mutants of either of the two alleles die around the late first-instar larval stage. Although cardiac structures such as ostia (hemolymph inflow tracts) still form, the number of cardioblasts is reduced, reflected by fewer than four non-ostia cardioblasts in each hemisegment (Fig. 3D-F). These results indicate that *Nedd4* is necessary to generate the expected numbers of cardioblasts.

Misexpression of *Nedd4* disrupts the patterning of cardioblasts and ostia cells in the adult fly hearts

As *Nedd4* and *miR-1* are both expressed in the developing fly heart, we speculated that *miR-1* might modulate the absolute levels of *Nedd4* within the fly heart. To determine the sensitivity of the fly heart to *Nedd4* activity, we overexpressed *Nedd4* in the heart using *twist-GAL4* or *Hand-GAL4* drivers (Han and Olson, 2005). Interestingly, using these *UAS-GAL4* systems (Brand and Perrimon, 1993) to misexpress wild-type (*UAS-Myc-Nedd4*) and ubiquitin-ligase mutant forms of *Nedd4* [*UAS-Myc-Nedd4(C/A)*], as well as *Nedd4*-RNAi, within the developing mesoderm permitted the recovery of adult flies (Fig. 4). Close examination of first-instar larvae revealed mild defects in the arrangement of the four pairs of Tinman-positive cardioblasts separated by two pairs of ostial cells (Fig. S4A,B). At 29°C, *Hand>UAS-Myc-Nedd4*, *Hand>UAS-Myc-Nedd4(C/A)* and *Hand>UAS-Nedd4-RNAi* animals had mildly reduced survival to eclosion and reduced adult life expectancy compared with control lines (n=60 for each genotype; Fig. S4C,D).

Development (2017) 144, 866-875 doi:10.1242/dev.140368

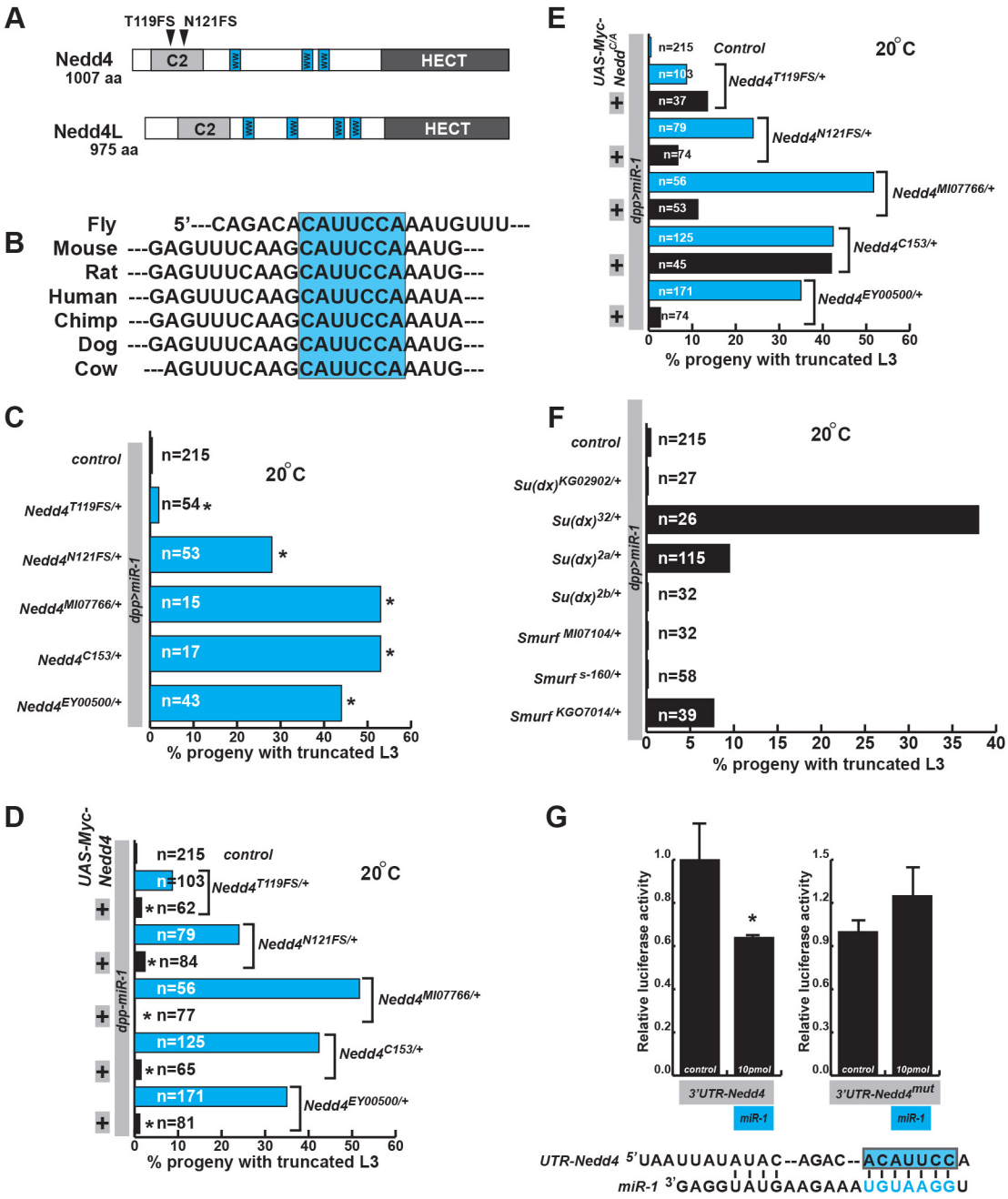

Fig. 2. *Nedd4* genetically interacts with *miR-1*, resulting in a truncated L3. (A) A structural schematic of Nedd4 with the tested mutations *Nedd4*^{MI07766}, *Nedd4*^{C153} and *Nedd4*^{EY00500} alleles are p-element insertions in upstream non-coding regions and are not depicted. Not drawn to scale. C2, Ca^{2+}-dependent phospholipid binding domain; HECT, catalytically active ubiquitin ligase domain; WW, substrate selection and cellular localization domain. (B) Schematic of the 3′UTR of *Nedd4* from various species; the conserved predicted *miR-1* target sequence is highlighted in blue. (C) Number of flies lacking the distal region of L3 by genotype (performed at 20°C). **P*<0.001. *n*, number of flies scored. (D) Genetic rescue studies. Graph shows the percentage of affected offspring for the noted crosses (performed at 20°C). The loss of L3 is less penetrant when wild-type *Nedd4* is co-expressed with *miR-1*. **P*<0.001. *n*, number of flies scored. (E) Genetic rescue studies as in D using a mutant form of Nedd4 lacking a functional HECT domain. Number of flies lacking the distal region of L3 by genotype (performed at 20°C). *n*, number of flies scored. In some genetic backgrounds, a functional HECT domain is not required for suppression of the vein truncation phenotype. (F) As in C. The Nedd4 family members Su(dx) and Smurf produce L3 truncation in selected genetic backgrounds. (G) Luciferase activity in transfected C2C12 (murine myoblast) cells of a reporter construct containing the 3′UTR of *Nedd4* (left) or a reporter construct with a deletion of the predicted *miR-1*-binding element (right).**P*≤0.05. (Bottom) Schematic showing base pairing of *Nedd4* mRNA with *miR-1*. Blue font indicates the *miR-1* seed sequence. Blue box indicates residues that were deleted to disrupt *miR-1* sensitivity and tested (right-hand bars).

Altered *Nedd4* expression caused pericardial cells to detach from mature fly hearts

To determine whether these modest disruptions in the normal patterning of first instar larvae resulted in morphological defects in the adult heart, we collected newly eclosed (adult) mutant fly hearts harboring the *Hand>UAS-Myc-Nedd4*, *Hand>UAS-Myc-Nedd4 (C/A)* or *Hand>UAS-Nedd4-RNAi* constructs. Individual hearts were fixed and stained with phalloidin to visualize the structure of the cardiac actin filaments. Pericardial cells were marked with *Hand*-GFP; an anti-pericardin antibody labeled the extracellular

Development (2017) 144, 866-875 doi:10.1242/dev.140368

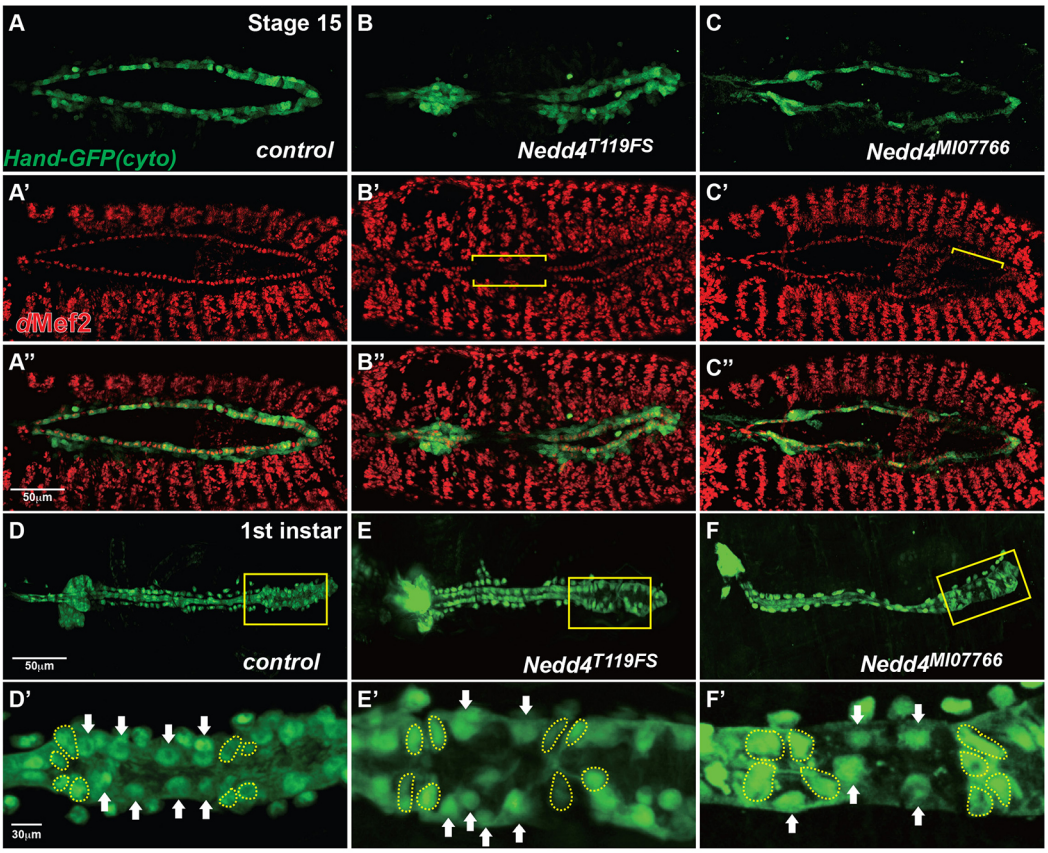

Fig. 3. *Nedd4* is required for normal patterning of the *Drosophila* heart. (A-C) Stage 15 *Nedd4*-null embryos marked by a *Hand-GFP* (cytoplasmic) construct to visualize cardioblasts and pericardial cells (green), with the genotype indicated in the lower right-hand corner. Anterior is towards the left. (A′-C′) Embryos stained with antibodies against Mef2 (*Drosophila* myocyte enhancer factor 2), a muscle marker (red), compared with representative *Nedd4*^{T119FS} and *Nedd4*^{MI07766} embryos with areas of reduced numbers of cardioblasts (yellow brackets). Genotypes as in A-C. (A″-C″) Overlay of A-C with A′-C′. (D-F) First-instar larvae with genotypes indicated in the bottom right-hand corner. Anterior is towards the left. (D′-F′) Higher magnification (20×) of the area highlighted by the yellow boxes in D-F, with ostial cells outlined by dashed lines and cardioblasts indicated by white arrows. Normally there are four cardioblasts between each set of four ostial cells; in *Nedd4*^{T119FS} and *Nedd4*^{MI07766} mutant larvae, the localization and/or number of these cardioblasts is abnormal. *n*=6 per phenotype.

matrix of the heart tube. Interestingly, compared with wild-type controls, animals with supraphysiological expression of *Nedd4* or the catalytically inactive form of *Nedd4* [*Nedd4(C/A)*] showed a dramatic increase in the number of detached pericardial cells, generalized disorganization of cardiac actin filaments (Fig. 4A-D) and a loss of cardiac muscle-fiber density (Fig. 4E). This phenotype is strikingly similar to other cardiac extracellular-matrix mutants, such as *Lonely heart* (*loh*) (Drechsler et al., 2013). To determine whether pericardial cells detached in the context of abnormal extracellular-matrix formation, we stained the flies for pericardin, a type IV collagen that is crucial for maintaining cardiac integrity in *Drosophila*. Consistent with a role for *Nedd4* for normal cardiac extracellular-matrix formation, we observed increased pericardin deposition in flies overexpressing *Hand>UAS-Myc-Nedd4(C/A)*, which expresses catalytically inactive *Nedd4* (Fig. 4C″). These results indicate that *Nedd4* may help maintain the normal myofibrillar structure of the heart tube and its associated pericardial cells. We propose that some of its effects on heart structure may be secondary to changes in pericardin deposition.

Changes in muscle fiber-associated actin filaments induced by overexpression of *miR-1* can be rescued by increasing expression of Nedd4 during larval stages

To determine whether abnormalities in heart structure or function induced by overexpression of *miR-1* could be genetically rescued by concurrent Nedd4 overexpression, we generated animals that concurrently overexpress *miR-1* and Nedd4 or Nedd4(C/A) [*Hand>UAS-Myc-Nedd4+UAS-miR-1*, *Hand>UAS-Myc-Nedd4 (C/A)+UAS-miR-1*]. Animals were raised at 20°C and pertinent progeny evaluated. We did not recover adult animals when *miR-1* was overexpressed, regardless of Nedd4 expression, indicating that overexpression of Nedd4 does not completely rescue abnormalities induced by excessive *miR-1* expression. By contrast, we were able to detect viable larvae, suggesting that genetic rescue may occur at earlier developmental stages. To visualize larval hearts, individual animals were fixed and stained with phalloidin to visualize the structure of the cardiac actin filaments. Overexpression of *miR-1* universally resulted in profound disorganization of the actin structures compared with wild type (Fig. 5B). Surprisingly, we found that, at L3, overexpression of Nedd4 and, to a lesser extent, Nedd4(C/A) was able to reduce the myofibrillar disorganization induced by overexpression of *miR-1*. These results indicate that, in larval heart, increasing Nedd4 expression can normalize actin fiber organization induced by excessive *miR-1* expression.

Nedd4L and *miR-1* levels are inversely proportional in mammalian hearts

These *in vivo* results prompted us to determine whether *miR-1* and *Nedd4l* interact genetically and biochemically in the mammalian heart. As with the luciferase assays testing the 3′UTR of *Nedd4* for

Development (2017) 144, 866-875 doi:10.1242/dev.140368

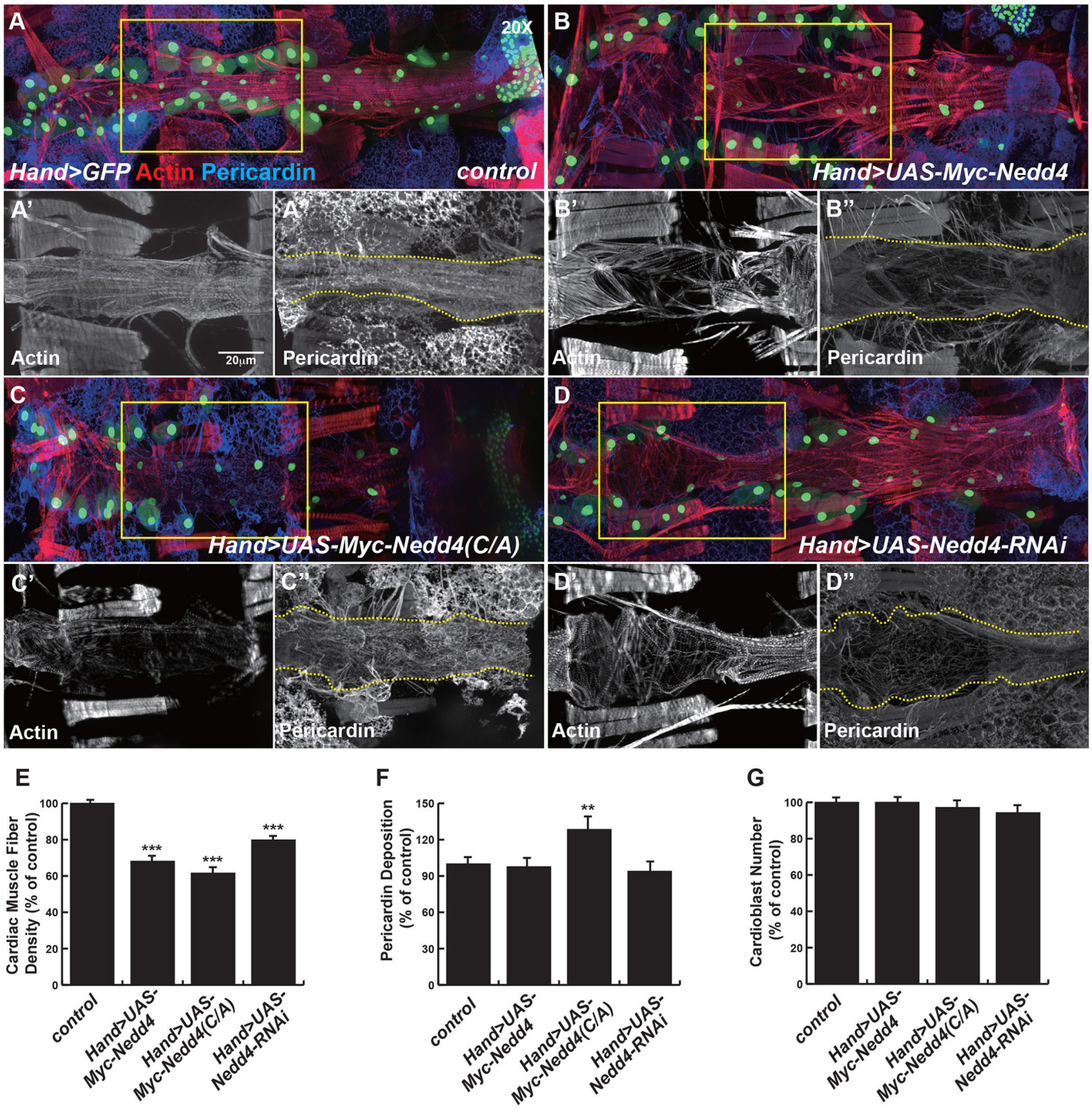

Fig. 4. Misexpression of Nedd4 in cardioblasts results in actin-fiber disarray and abnormal pericardin deposition. (A-D) Newly eclosed adult flies harboring a *Hand-GFP* (cytoplasmic) construct to visualize pericardial cells (green) with muscle-associated actin filaments (red) and pericardin (blue). Genotype is indicated in the lower right corner. Anterior is towards the left. (A′-D′) Higher magnifications (20×) of areas outlined by the yellow boxes in A-D, demonstrating the normal arrangement of actin filaments (A′) versus the disarrayed actin fibers seen in *Hand>UAS-Myc-Nedd4*, *Hand>UAS-Myc-Nedd4(C/A)* and *Hand>UAS-Nedd4-RNAi* (B′-D′). (A″-D″) As for A′-D′ with the heart tube outlined (dashed line) where pericardin deposition was quantified. *n*=3 per phenotype. (E) Quantification of cardiac muscle-fiber density by genotype, normalized to wild type. ****P*<0.01. (F) Quantification of pericardin staining in the heart tube area as outlined in A″-D″. **P*<0.05. (G) Quantification of cardioblast number by genotype.

miR-1 sensitivity, the 3′UTR of *Nedd4l* was also sensitive to *miR-1* regulation (Fig. 6A). To determine whether the expression of Nedd4L was inversely proportional to *miR-1* levels in murine hearts, we took advantage of the fact that *miR-1* levels rise after birth as part of the transition from the fetal to the postnatal circulation (Fig. 6B). We postulated that during this postnatal period, as *miR-1* levels physiologically increase, Nedd4L levels would fall. To test this hypothesis, we performed western blot analysis on whole-heart lysates obtained from wild-type mice at postnatal days 2 and 21 (P2 and P21) using anti-Nedd4L antibodies (Bethyl). Each postnatal period was represented by a minimum of five individual hearts, and the amounts of Nedd4L were normalized to the GAPDH loading

Development (2017) 144, 866-875 doi:10.1242/dev.140368

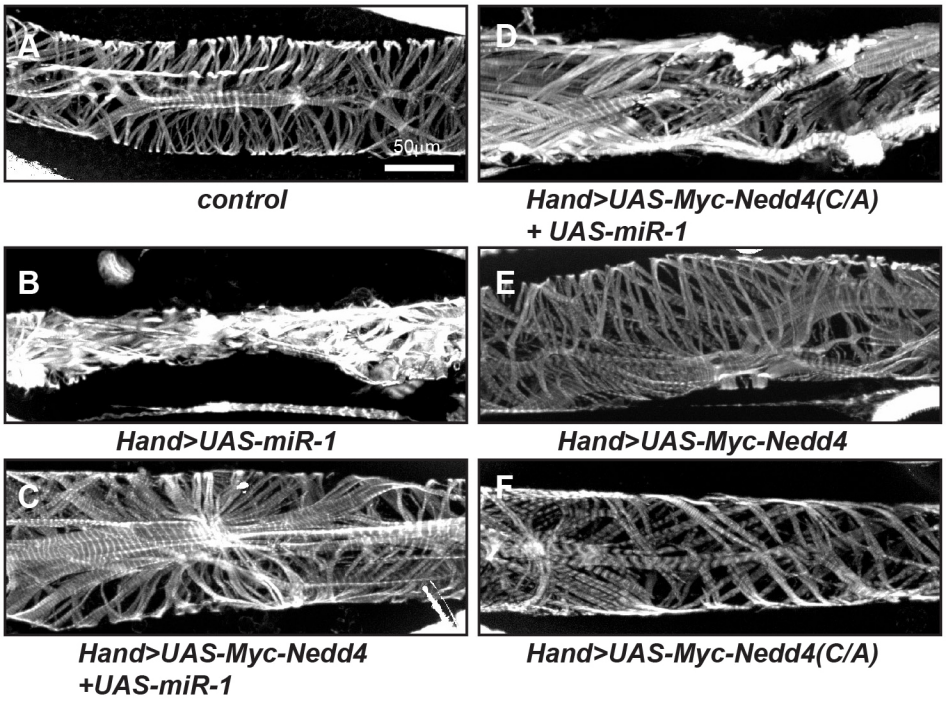

Fig. 5. Overexpression of Nedd4 is able to rescue *miR-1*-mediated actin fiber disarray in larval hearts. (A) Wild-type larval (L3) heart stained with muscle-associated actin filaments. (B) Overexpression of *miR-1* in the fly heart using the *Hand>UAS-miR-1* expression construct results in actin filament disorganization and collapse. (C) Concurrent expression of Nedd4 with *miR-1* (*Hand>UAS-Myc-Nedd4+UAS-miR-1*) significantly normalizes actin fiber organization. (D) Concurrent expression of a ubiquitin ligase-deficient mutant of Nedd4 with *miR-1* [*Hand>UAS-Myc-Nedd4(C/A)+UAS-miR-1*] improves actin fiber organization. (E,F) Overexpression of Nedd4 (*Hand>UAS-Myc-Nedd4*) or mutant Nedd4 [*Hand>UAS-Myc-Nedd4(C/A)*] in larval hearts has minimal effects on actin fiber organization. All larvae were raised at 29°C. *n*=6 for each genotype.

control. We found that the levels of Nedd4L expression were ∼2.5-fold higher in P2 hearts compared with P21 hearts. Based on these results, we investigated whether Nedd4L expression was perturbed in *miR-1* null (*miR-1-1*$^{-/-}$*; miR-1-2*$^{-/-}$) mice. We performed a targeted analysis of data from RNA sequencing of heart lysates from late embryonic (E18) *miR-1* null (*miR-1-1*$^{-/-}$*; miR-1-2*$^{-/-}$) mice versus wild-type controls (Heidersbach et al., 2013). Consistent with a model in which *miR-1* directly targets *Nedd4l*, *miR-1*-null hearts had significantly increased levels of *Nedd4l* mRNA (Fig. 6D). To determine whether this increase in Nedd4L RNA altered protein expression, we analyzed lysates of P2 murine heart cells by western blot (Fig. 6E). In wild-type P2 hearts, Nedd4L levels were low but detectable. By contrast, *miR-1*-null mice had significantly increased Nedd4L levels at the predicted molecular weight, plus two additional bands (*n*=3 per genotype), as seen in the wild-type hearts. Nedd4L levels in *miR-1*-null mice at P21 could not be determined, because the *miR-1* null state is lethal by P7 owing to heart failure. In summary, these results support the hypothesis that *miR-1* regulates *Nedd4l* to affect the physiology of the mammalian heart.

DISCUSSION

Unexpectedly, we found that overexpression of *miR-1* in the anterior-posterior (AP) organizer of the wing disc results in a dose-dependent loss of L3 vein structures, consistent with de-repression of Notch or weakening of a regulatory mechanism that dampens the Notch signal. Using genetic techniques, we determined that the loss of the distal aspect of L3 could be phenocopied by reducing the gene dose of Notch co-repressors or *Nedd4*; in the case of *Nedd4*, the regulation by *miR-1* was direct. We propose an expanded model in which *miR-1* expression in the AP organizer has complex effects on Notch signaling owing to its regulation of ligand availability and receptor trafficking. As lower levels of *miR-1* expression (18°C) caused wing-vein thickening and tortuosity, and higher levels (22°C) caused vein loss, Delta and Nedd4 may be differentially sensitive to *miR-1* regulation, although our studies were not designed to address this issue. It is also possible that indirect effects, such as reductions in Nedd4-mediated ubiquitylation of positive effectors of the Notch receptor (e.g. Deltex) or perturbations in Delta-mediated *cis*-inhibition, contributed to the de-repression of Notch in our wing-based assay system.

Our findings in the mammalian heart indicate that the genetic and biochemical interaction between *miR-1* and *Nedd4l* is physiologically relevant and may provide developmental or tissue-specific regulation of *Nedd4l* in the myocardium. We speculate that the additional bands observed on western blots of heart lysates using an anti-Nedd4L antibody might result from post-translational modifications, because Nedd4L can autoregulate its stability through ubiquitylation of its HECT domain (Bruce et al., 2008). Alternatively, they might represent heart-specific splice variants, because tissue-specific isoforms of Nedd4L have been found in the heart and the liver (Chen et al., 2001; Fu et al., 2013).

Importantly, although *miR-1*-mediated reductions in Nedd4 activity caused wing-vein phenotypes induced by Notch, *miR-1*-mediated dysregulation of Nedd4L in the heart likely affects proteins outside the Notch pathway. Indeed, protein microarrays comparing human Nedd4 with human Nedd4L, suggest that Nedd4L (also known as Nedd4-2) preferentially targets ion channels, whereas Nedd4 targets are enriched for signaling pathways (Persaud et al., 2009). Thus, in the heart, where *miR-1* and murine Nedd4L are both expressed, their genetic and biochemical interaction might influence the excitability and connectivity of cardiomyocytes. Indeed, susceptibility to cardiac arrhythmias and sudden death in humans is associated with six genes that encode ion channels (*SCN5A*, *KCNQ1*, *KCNH2*, *KCNE1*, *KCNE2* and *RYR2*) (reviewed by Keating and Sanguinetti, 2001). Murine Nedd4L regulates the cell-surface densities of the sodium channel, the voltage-gated type V alpha subunit (Scn5a) (Abriel et al., 2000; Rougier et al., 2005; van Bemmelen et al., 2004), the potassium voltage-gated channel, KQT-like subfamily member 1 (Kcnq1) (Jespersen et al., 2007; Krzystanek et al., 2012) and the human Ether-a-go-go-related (KCNH2, previously hERG) channel (Albesa et al., 2011; Guo et al., 2012). Furthermore, *miR-1* directly regulates human KCNJ2, a channel that maintains cardiac resting potential (Yang et al., 2007). These findings suggest that

Development (2017) 144, 866-875 doi:10.1242/dev.140368

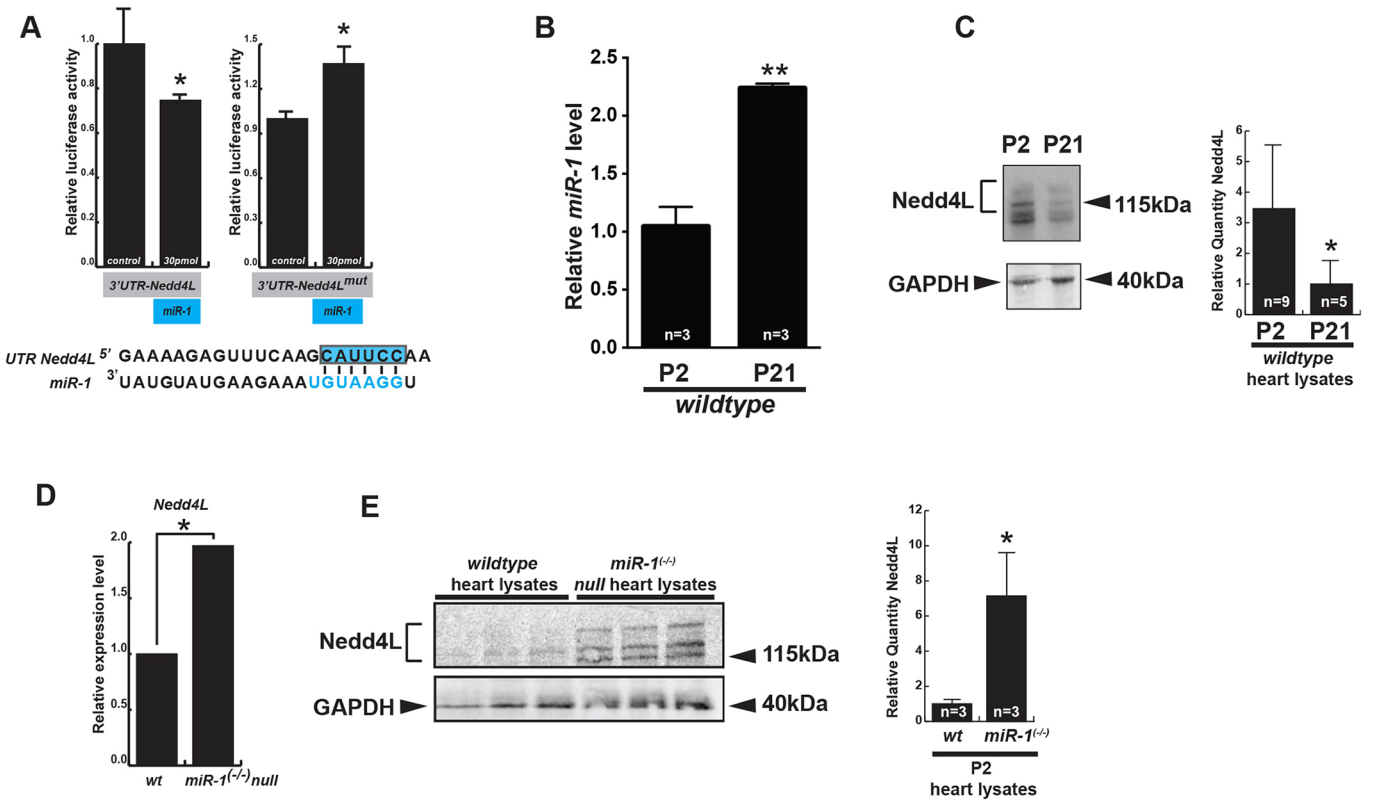

Fig. 6. Regulation of Nedd4 by *miR-1* is evolutionarily conserved. (A) (Top) Luciferase activity is shown in transfected C2C12 (murine myoblast) cells of a reporter construct containing the 3′UTR of murine *Nedd4l* (left) or a deletion of the predicted *miR-1* binding element (right). *$P \leq 0.05$. (Bottom) A schematic showing base pairing of *Nedd4l* mRNA with *miR-1*. Blue font indicates the *miR-1* seed sequence. Blue box indicates deleted residues that disrupted *miR-1* sensitivity, as tested in the above panels. (B) qRT-PCR demonstrating changes in *miR-1* expression postnatally. *miR-1* levels were normalized to Sno202. **$P<0.01$; P, postnatal day. (C) (Left) Representative western blot of whole heart-cell lysates from wild-type postnatal day (P) 2 and P21 mice. (Right) Quantification of band intensity for Nedd4L protein normalized to GAPDH. *$P<0.05$. *n*, number of hearts. (D) Relative expression levels determined by RNA sequencing of *Nedd4l* transcripts in wild-type versus *miR-1*$^{-/-}$ hearts at embryonic stage 18 (E18). *$P<0.05$. (E) (Left) Western blot of Nedd4L in heart lysates from postnatal day 2 (P2) from wild-type or *m-miR-1*$^{-/-}$ mice (*n*=3 per genotype). GAPDH served as a loading control. (Right) Quantification of band intensity for Nedd4L protein normalized to GAPDH. *$P<0.05$. *n*, number of hearts.

the regulation of murine *Nedd4l* by *miR-1* contributes to some of the electrophysiological abnormalities seen in *miR-1* null mice (Heidersbach et al., 2013; Wei et al., 2014; Zhao et al., 2007). It would be interesting to determine whether Nedd4L is dysregulated in the heart after an infarction or under ischemic conditions, when *miR-1* is upregulated and fatal cardiac dysrhythmias are common.

MATERIALS AND METHODS

Fly stocks

Drosophila lines were obtained from Bloomington Stock Center (NIH P40OD018537). The following fly lines were generously provided by G. Tear (King's College London, UK): *Nedd4*^{T119FS}, *Nedd4*^{N121FS} and *UAS-Nedd4* (Myat et al., 2002). *W*^{1118} flies served as wild-type controls. Transgenes were overexpressed with the *UAS-GAL4* system (Brand and Perrimon, 1993). The following *GAL4* and *UAS* lines were used: *dpp-GAL4* (Bloomington Stock Center) and *UAS-miR-1* (C. Kwon, Johns Hopkins University, Baltimore, MD, USA) (Kwon et al., 2005). The *Ellipse* allele (*Elp*^{B1}) was provided by G. Rubin (HHMI Janelia Research Campus, VA, USA) (Baker and Rubin, 1989).

Wing imaging

Adult *Drosophila* were anesthetized with CO_2, placed in isopropanol for 1 min and euthanized. Flies were air dried, their wings were removed and embedded in Canada Balsam (Sigma), and covered with a glass coverslip. Images were taken on a LeicaMZ16F microscope at 5× magnification with a Leica DFC310FX camera and the Leica Application Suite (LAS) program. Images were processed using Adobe Photoshop CS6 and the white set-point function was used for background lightening.

Drosophila embryonic imaging

Embryos were collected and stained with various antibodies as previously described (Han and Olson, 2005). Rabbit anti-Dmef2 was used at 1:1000 dilution. Cy3, Cy5 or biotin-conjugated secondary antibodies (from Jackson Labs) were used. Adult flies were dissected and fixed for 10 min in 4% paraformaldehyde in phosphate-buffered saline (PBS). Alexa Fluor R555 phalloidin was obtained from Thermo Fisher. Mouse anti-pericardin antibody (EC11) was used at 1:500 dilution, followed by Cy3-conjugated secondary antibodies (Jackson Labs). Confocal imaging was performed with a Zeiss ApoTome.2 microscope using a 20× Plan-Apochromat 0.8 N.A. air objective. For quantitative comparisons of intensities, common settings were chosen to avoid oversaturation. ImageJ Software Version 1.49 was used to process images.

Drosophila larval and adult heart imaging

Larvae and adult flies were dissected and fixed for 10 min in 4% paraformaldehyde in phosphate-buffered saline (PBS). Alexa Fluor 555 phalloidin was obtained from Thermo Fisher. Mouse anti-pericardin antibody (EC11) was used at 1:500 dilutions, followed by Cy3-conjugated secondary antibodies (Jackson Labs). Confocal imaging was performed with a Zeiss ApoTome.2 microscope using a 20× Plan-Apochromat 0.8 N.A. air objective. For quantitative comparisons of intensities, common settings were chosen to avoid oversaturation. A minimum of 6 larvae or adults per genotype were visualized. ImageJ

Development (2017) 144, 866-875 doi:10.1242/dev.140368

Software Version 1.49 was used for image processing. For quantitative comparisons of cardiac muscle fiber density, cardioblast cell numbers and pericardin deposition we analyzed six control flies and six flies of each experimental genotype. Sample size determinations were based upon extensive previous experience of mutant fly heart morphological analysis.

Fly survival assay

On day 6 after egg laying, *Drosophila* larvae were transferred from 25°C to 29°C to enhance the temperature-sensitive UAS-transgene expression. Adult male flies were subsequently maintained at 29°C in vials containing 15 or animals. Sixty flies were assayed per genotype.

Luciferase assay

Approximately 200 base pairs surrounding the predicted *miR-1*-target sites in the untranslated regions (UTRs) of *Nedd4* or *Nedd4l* were amplified directly from cDNA generated from W^{1118} flies or wild-type mouse hearts, respectively, and subcloned with *Xba*I into the PGL3 (Promega) firefly luciferase vector at the 3′ end of the reporter gene. Correct insertion was confirmed by sequencing.

For transfection of the C2C12 murine myoblast cell line (ATCC) with luciferase constructs and a Renilla normalization vector, we used Lipofectamine 2000 (Life Technologies) according to the manufacturer's instructions. Briefly, cells in 12-well plates were transfected at 60% confluency and analyzed 20 h later. Each well received 3 µl of Lipofectamine 2000, 800 ng of PGL3-Target and 200 ng of Renilla vector. Experimental wells received 10 pmol of *miR-1* mimic (Ambion/Life Technologies), and control wells received 10 pmol of a non-targeting control mimic (Ambion/Life Technologies).

Firefly and Renilla luciferase activities in lysates were quantified with the Dual Luciferase Reporter Assay kit (Promega) and a Victor 1420 Multilabel Counter (PerkinElmer). Firefly luciferase values were normalized to Renilla to control for transfection efficiency.

RNA sequencing

Whole hearts from embryonic day 18 (E18) wild-type and *miR-1* double-knockout mice were isolated and analyzed as described previously (Heidersbach et al., 2013).

Quantitative PCR

Postnatal hearts were obtained from C57BL/6J pups after timed matings, with n=3 at each time point. Animals were sacrificed by CO_2 asphyxiation followed by decapitation. Hearts were snap frozen in liquid nitrogen and subsequently transferred to Trizol (ThermoFisher Scientific) and homogenized in a Bullet Blender using 2 mm ZrSiO beads, according to the manufacturer's instructions (Next Advance). RNA was isolated using the Direct-zol RNA MiniPrep kit (catalog number R2052) from Zymo Research. cDNA was prepared using a High Capacity cDNA Reverse Transcription Kit (catalog number 4368814) and *miR-1* TaqMan probes (catalog number 4427975) from Thermo Fisher. *miR-1* levels were normalized to *SnoRNA-202* (catalog number 427975) according to manufacturer's recommendations. Mice of both sexes were housed under the UCSF 'Assurance of Compliance with PHS Policy on Humane Care and Use of Laboratory Animals by Awardee Institutions', and their use was approved by the UCSF Institutional Animal Care and Use Committee.

Western blots

Hearts were isolated from mice on postnatal days 2 and 21 (P2, P21) and rinsed with 1× PBS. The tissue was resuspended in RIPA buffer and disassociated in a Bullet Blender using 2 mm ZrSiO beads according to the manufacturer's instructions (Next Advance). After clarification and sonication, the lysates were loaded onto a 4-12% SDS-PAGE gel (Biorad), blotted onto polyvinylidene fluoride (PDVF) membranes by standard protocols, and probed with primary antibodies against GAPDH (Abcam; 1:5000) and Nedd4L (Bethyl A302-512A; 1:2000). Blots were visualized and quantified with a Licor Odyssey system and fluorescently conjugated secondary antibodies (Licor, Lincoln, NE), according to the manufacturer's instructions.

Statistics

The rates of genetic enhancement or truncation of long vein 3 (L3) were analyzed with the chi-square test. Mean, s.d. and s.e.m. were calculated for luciferase assays. qRT-PCR of relative *miR-1* levels were performed with GraphPad Prism (version 6.0) for *t*-tests. Differences between two means were assessed by two-tailed *t*-tests, unless otherwise stated. Error bars represent s.e.m. Null hypotheses were rejected at $P<0.05$.

Acknowledgements

We thank Gary Howard, Stephen Ordway, Adam Richman, Crystal Herron and Bethany Taylor for editorial assistance, Karen Carver-Moore and Lei Liu for mouse colony support, and Joshua Urrutia for technical support.

Competing interests

The authors declare no competing or financial interests.

Author contributions

I.N.K. designed and performed the *Drosophila* wing assay and conducted western blotting on wild-type mouse hearts. J.-y.Z. and Z.H. performed the misexpression analysis, rescue studies of the fly heart and fly mortality studies. A.H., K.N.I. and D.S. generated the *miR-1*-null mice. A.H. performed the western blot on the *miR-1*-null heart cell lysates and the luciferase assays. I.S.K. and B.I.G. obtained and determined the *miR-1* levels from wild-type murine hearts. Z.H. and I.N.K. wrote the manuscript.

Funding

This work was supported by a Mentored Research Training Grant from the Foundation for Anesthesia Education and Research (I.S.K.), by the National Institutes of Health (NIH) (R01 HL057181 to D.S., K08 HL079260, R01HL090801 and R01DK098410), by the American Heart Association (AHA-0630178N to Z.H.) and by a Basil O'Connor Starter Scholar Research Award (5-FY10-489) from the March of Dimes Foundation to I.N.K. Deposited in PMC for release after 12 months.

Supplementary information

Supplementary information available online at
http://dev.biologists.org/lookup/doi/10.1242/dev.140368.supplemental

References

Abriel, H., Kamynina, E., Horisberger, J.-D. and Staub, O. (2000). Regulation of the cardiac voltage-gated Na^+ channel (H1) by the ubiquitin-protein ligase Nedd4. *FEBS Lett.* **466**, 377-380.

Albesa, M., Grilo, L. S., Gavillet, B. and Abriel, H. (2011). Nedd4-2-dependent ubiquitylation and regulation of the cardiac potassium channel hERG1. *J. Mol. Cell. Cardiol.* **51**, 90-98.

Baker, N. E. and Rubin, G. M. (1989). Effect on eye development of dominant mutations in Drosophila homologue of the EGF receptor. *Nature* **340**, 150-153.

Brand, A. H. and Perrimon, N. (1993). Targeted gene expression as a means of altering cell fates and generating dominant phenotypes. *Development* **118**, 401-415.

Bruce, M. C., Kanelis, V., Fouladkou, F., Debonneville, A., Staub, O. and Rotin, D. (2008). Regulation of Nedd4-2 self-ubiquitination and stability by a PY motif located within its HECT-domain. *Biochem. J.* **415**, 155-163.

Casso, D. J., Biehs, B. and Kornberg, T. B. (2011). A novel interaction between hedgehog and Notch promotes proliferation at the anterior-posterior organizer of the Drosophila wing. *Genetics* **187**, 485-499.

Chen, H., Ross, C. A., Wang, N., Huo, Y., MacKinnon, D. F., Potash, J. B., Simpson, S. G., McMahon, F. J., DePaulo, J. R., Jr and McInnis, M. G. (2001). NEDD4L on human chromosome 18q21 has multiple forms of transcripts and is a homologue of the mouse Nedd4-2 gene. *Eur. J. Hum. Genet.* **9**, 922-930.

de Celis, J. F. and García-Bellido, A. (1994). Roles of the Notch gene in Drosophila wing morphogenesis. *Mech. Dev.* **46**, 109-122.

Drechsler, M., Schmidt, A. C., Meyer, H. and Paululat, A. (2013). The conserved ADAMTS-like protein lonely heart mediates matrix formation and cardiac tissue integrity. *PLoS Genet.* **9**, e1003616.

Easow, G., Teleman, A. A. and Cohen, S. M. (2007). Isolation of microRNA targets by miRNP immunopurification. *RNA* **13**, 1198-1204.

Fu, J., Akhmedov, D. and Berdeaux, R. (2013). The short isoform of the ubiquitin ligase NEDD4L is a CREB target gene in hepatocytes. *PLoS ONE* **8**, e78522.

Guo, J., Wang, T., Li, X., Shallow, H., Yang, T., Li, W., Xu, J., Fridman, M. D., Yang, X. and Zhang, S. (2012). Cell surface expression of human ether-a-go-go-related gene (hERG) channels is regulated by caveolin-3 protein via the ubiquitin ligase Nedd4-2. *J. Biol. Chem.* **287**, 33132-33141.

Han, Z. and Olson, E. N. (2005). Hand is a direct target of Tinman and GATA factors during Drosophila cardiogenesis and hematopoiesis. *Development* **132**, 3525-3536.

Hasson, P., Egoz, N., Winkler, C., Volohonsky, G., Jia, S., Dinur, T., Volk, T., Courey, A. J. and Paroush, Z. (2005). EGFR signaling attenuates Groucho-dependent repression to antagonize Notch transcriptional output. *Nat. Genet.* **37**, 101-105.

Heidersbach, A., Saxby, C., Carver-Moore, K., Huang, Y., Ang, Y.-S., de Jong, P. J., Ivey, K. N. and Srivastava, D. (2013). microRNA-1 regulates sarcomere formation and suppresses smooth muscle gene expression in the mammalian heart. *Elife* **2**, e01323.

Ingham, R. J., Gish, G. and Pawson, T. (2004). The Nedd4 family of E3 ubiquitin ligases: functional diversity within a common modular architecture. *Oncogene* **23**, 1972-1984.

Itoh, M., Kim, C.-H., Palardy, G., Oda, T., Jiang, Y.-J., Maust, D., Yeo, S.-Y., Lorick, K., Wright, G. J., Ariza-McNaughton, L. et al. (2003). Mind bomb is a ubiquitin ligase that is essential for efficient activation of Notch signaling by Delta. *Dev. Cell* **4**, 67-82.

Ivey, K. N., Muth, A., Arnold, J., King, F. W., Yeh, R.-F., Fish, J. E., Hsiao, E. C., Schwartz, R. J., Conklin, B. R., Bernstein, H. S. et al. (2008). MicroRNA regulation of cell lineages in mouse and human embryonic stem cells. *Cell Stem Cell* **2**, 219-229.

Jespersen, T., Membrez, M., Nicolas, C. S., Pitard, B., Staub, O., Olesen, S. P., Baro, I. and Abriel, H. (2007). The KCNQ1 potassium channel is down-regulated by ubiquitylating enzymes of the Nedd4/Nedd4-like family. *Cardiovasc. Res.* **74**, 64-74.

Keating, M. T. and Sanguinetti, M. C. (2001). Molecular and cellular mechanisms of cardiac arrhythmias. *Cell* **104**, 569-580.

King, I. N., Qian, L., Liang, J., Huang, Y., Shieh, J. T. C., Kwon, C. and Srivastava, D. (2011). A genome-wide screen reveals a role for microRNA-1 in modulating cardiac cell polarity. *Dev. Cell* **20**, 497-510.

Krzystanek, K., Rasmussen, H. B., Grunnet, M., Staub, O., Olesen, S.-P., Abriel, H. and Jespersen, T. (2012). Deubiquitylating enzyme USP2 counteracts Nedd4-2-mediated downregulation of KCNQ1 potassium channels. *Heart Rhythm* **9**, 440-448.

Kwon, C., Han, Z., Olson, E. N. and Srivastava, D. (2005). MicroRNA1 influences cardiac differentiation in Drosophila and regulates Notch signaling. *Proc. Natl. Acad. Sci. USA* **102**, 18986-18991.

Myat, A., Henry, P., McCabe, V., Flintoft, L., Rotin, D. and Tear, G. (2002). Drosophila Nedd4, a ubiquitin ligase, is recruited by Commissureless to control cell surface levels of the roundabout receptor. *Neuron* **35**, 447-459.

Persaud, A., Alberts, P., Amsen, E. M., Xiong, X., Wasmuth, J., Saadon, Z., Fladd, C., Parkinson, J. and Rotin, D. (2009). Comparison of substrate specificity of the ubiquitin ligases Nedd4 and Nedd4-2 using proteome arrays. *Mol. Syst. Biol.* **5**, 333.

Rotin, D. and Kumar, S. (2009). Physiological functions of the HECT family of ubiquitin ligases. *Nat. Rev. Mol. Cell Biol.* **10**, 398-409.

Rotin, D., Staub, O. and Haguenauer-Tsapis, R. (2000). Ubiquitination and endocytosis of plasma membrane proteins: role of Nedd4/Rsp5p family of ubiquitin-protein ligases. *J. Membr. Biol.* **176**, 1-17.

Rougier, J.-S., van Bemmelen, M. X., Bruce, M. C., Jespersen, T., Gavillet, B., Apotheloz, F., Cordonier, S., Staub, O., Rotin, D. and Abriel, H. (2005). Molecular determinants of voltage-gated sodium channel regulation by the Nedd4/Nedd4-like proteins. *Am. J. Physiol. Cell Physiol.* **288**, C692-C701.

Sakata, T., Sakaguchi, H., Tsuda, L., Higashitani, A., Aigaki, T., Matsuno, K. and Hayashi, S. (2004). Drosophila Nedd4 regulates endocytosis of notch and suppresses its ligand-independent activation. *Curr. Biol.* **14**, 2228-2236.

Sokol, N. S. and Ambros, V. (2005). Mesodermally expressed Drosophila microRNA-1 is regulated by Twist and is required in muscles during larval growth. *Genes Dev.* **19**, 2343-2354.

van Bemmelen, M. X., Rougier, J.-S., Gavillet, B., Apothéloz, F., Daidie, D., Tateyama, M., Rivolta, I., Thomas, M. A., Kass, R. S., Staub, O. et al. (2004). Cardiac voltage-gated sodium channel Nav1.5 is regulated by Nedd4-2 mediated ubiquitination. *Circ. Res.* **95**, 284-291.

Wei, Y., Peng, S., Wu, M., Sachidanandam, R., Tu, Z., Zhang, S., Falce, C., Sobie, E. A., Lebeche, D. and Zhao, Y. (2014). Multifaceted roles of miR-1s in repressing the fetal gene program in the heart. *Cell Res.* **24**, 278-292.

Wilkin, M. B., Carbery, A.-M., Fostier, M., Aslam, H., Mazaleyrat, S. L., Higgs, J., Myat, A., Evans, D. A. P., Cornell, M. and Baron, M. (2004). Regulation of notch endosomal sorting and signaling by Drosophila Nedd4 family proteins. *Curr. Biol.* **14**, 2237-2244.

Yang, B. and Kumar, S. (2010). Nedd4 and Nedd4-2: closely related ubiquitin-protein ligases with distinct physiological functions. *Cell Death Differ.* **17**, 68-77.

Yang, B., Lin, H., Xiao, J., Lu, Y., Luo, X., Li, B., Zhang, Y., Xu, C., Bai, Y., Wang, H. et al. (2007). The muscle-specific microRNA miR-1 regulates cardiac arrhythmogenic potential by targeting GJA1 and KCNJ2. *Nat. Med.* **13**, 486-491.

Zhao, Y., Ransom, J. F., Li, A., Vedantham, V., von Drehle, M., Muth, A. N., Tsuchihashi, T., McManus, M. T., Schwartz, R. J. and Srivastava, D. (2007). Dysregulation of cardiogenesis, cardiac conduction, and cell cycle in mice lacking miRNA-1-2. *Cell* **129**, 303-317.

Figure S1:

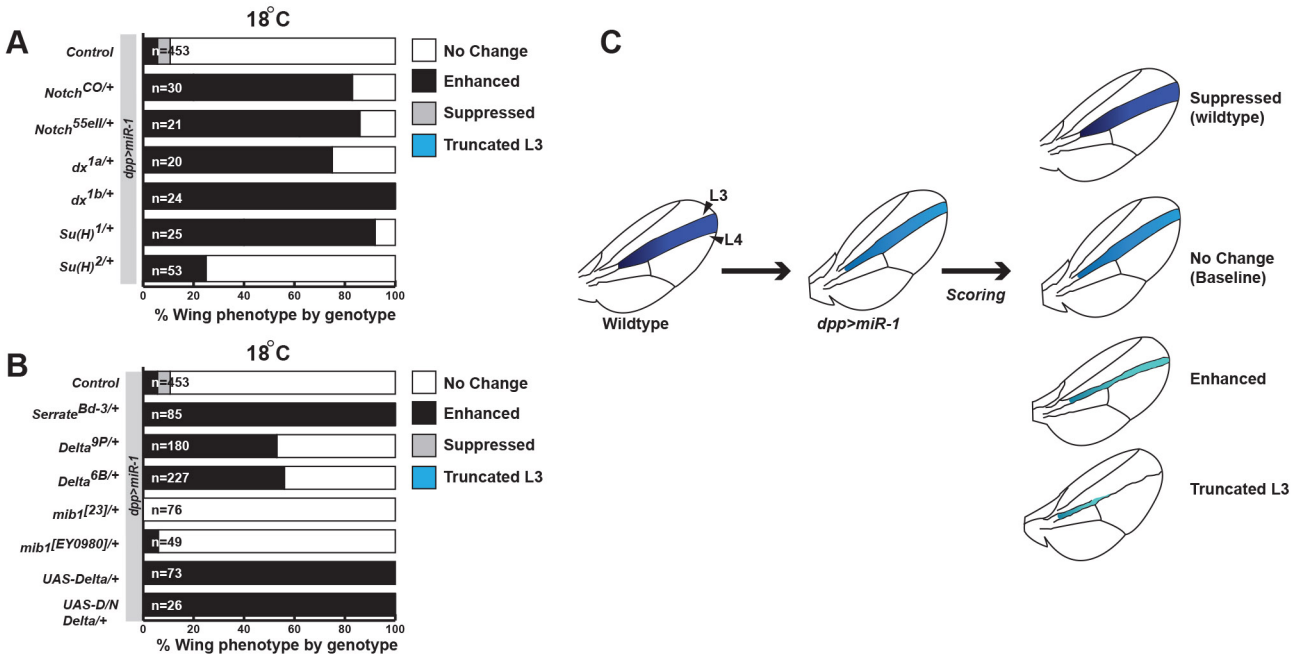

Fig. S1. Positive Effectors of Notch Signaling Do Not Mediate the Truncation of L3. (A) Percentage of progeny displaying "no change," "enhanced," "suppressed," or "truncated L3" by genotype when crossed to the *dpp>dmiR-1* line at 18°C. At this temperature, L3 is formed normally in the control *dpp>miR-1* line and loss of the L3-L4 intervein distance predominates. Note that no animals display the L3 truncation phenotype. n=number of progeny scored. (B) As in (A), with emphasis on the mutants of Notch ligands Delta and serrate and the regulator of Delta, mindbomb1. Control, *dpp>dmiR-1;* D/N Delta, dominant-negative Delta; dx, deltex; mib1, mindbomb1; Su(H), Suppressor of Hairless. (C) Schematic of the scoring system based on changes in the L3-L4 intervein distance observed with the *dpp>dmiR-1* fly line.

Figure S2:

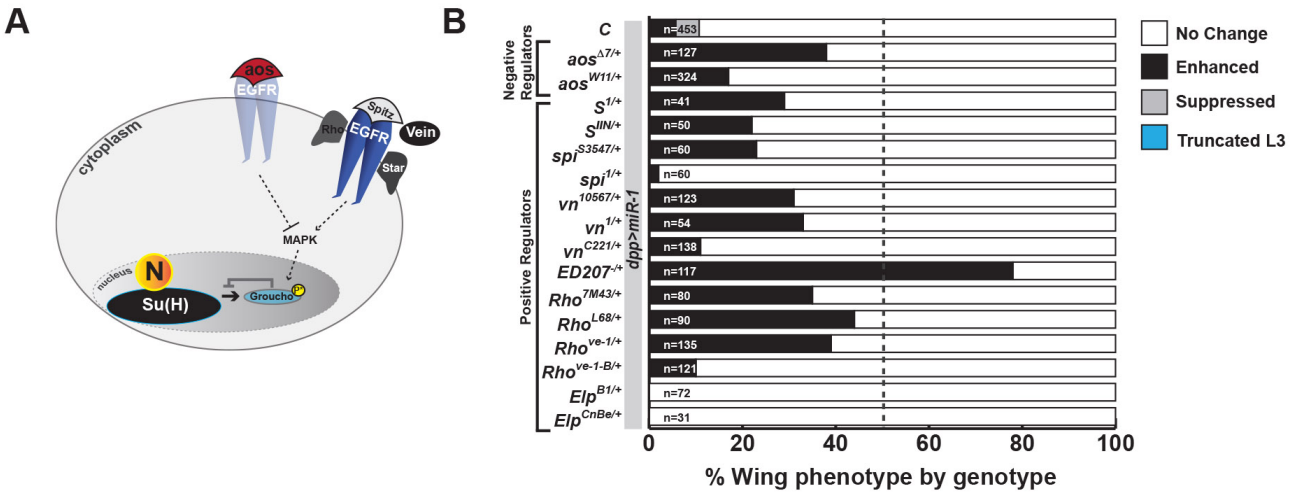

Fig. S2. Phosphorylation of Groucho does not Result in L3 truncation. (A) Schematic of Epidermal growth factor Receptor (EFGR) signaling as it pertains to the regulation of the Notch (N) repressor Groucho. (B) Genetic interaction studies. Graph shows the percentage of affected offspring for the noted crosses (performed at 18°C) for each of the possible alterations in L3-L4 intervein distance as depicted in. The loss of L3 does not occur for any of the stated crosses indicating that phosphorylation of Groucho does not play a significant role in the truncation of L3. n=number of flies scored. *C: control, aos:argos, S:star, Spi:spitz, vn: vein, Elp: elipse* (EGFR gain of function allele)

Figure S3:

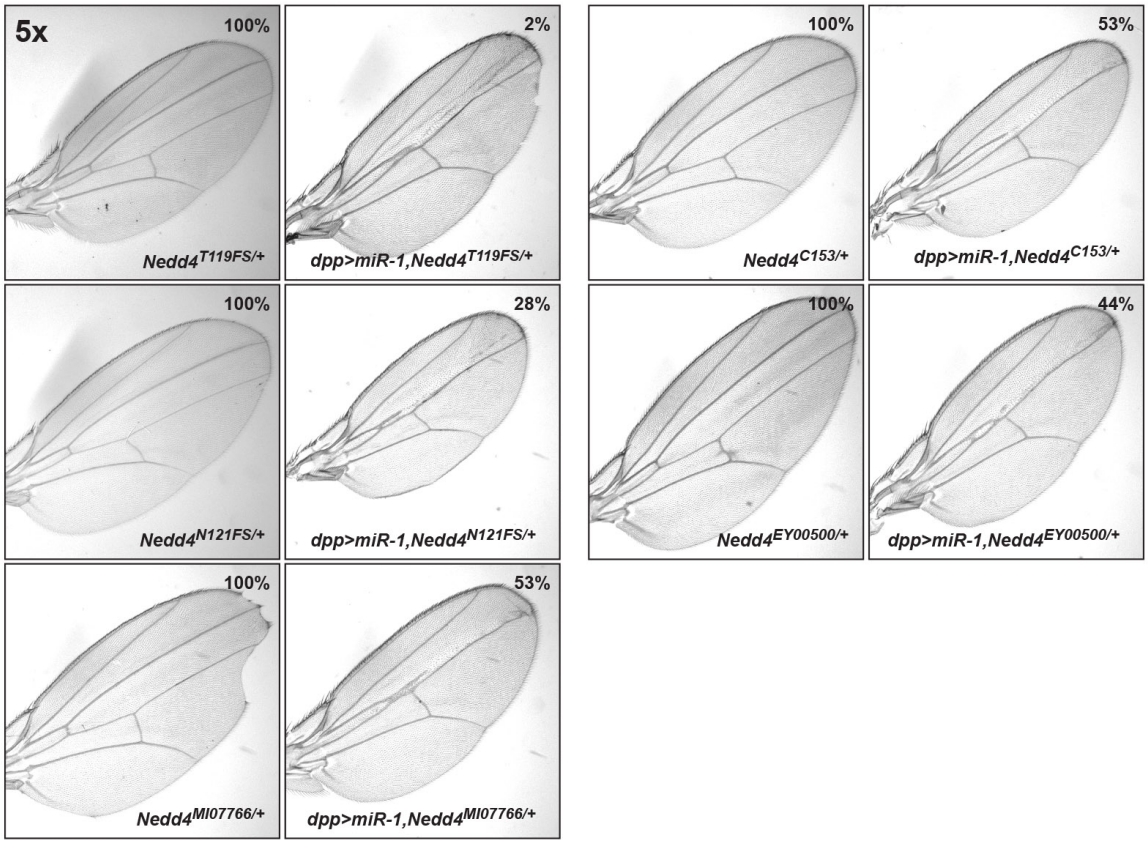

Fig. S3. *dNedd4* Genetically Interacts with *dmiR-1*, resulting in a Truncated L3. Representative wing morphology of control (parental) or *dpp>dmiR-1,dNedd4*$^{(-/+)}$ mutant progeny with L3 truncation were quantified as in Figure 2C. Genotypes are noted. Penetrance for each genotype is shown at top right.

Figure S4:

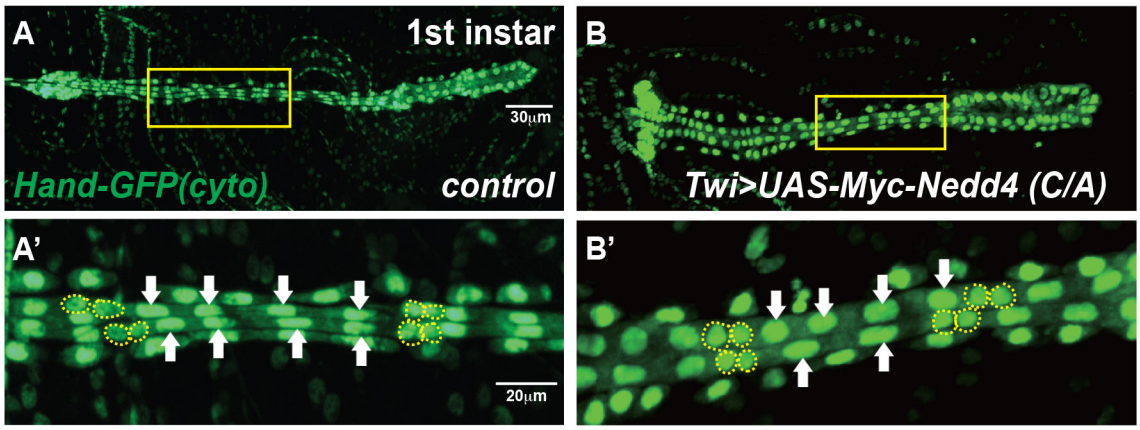

C

	X Hand-Gal4/Cyo		
	Curly wing (with CyO)	Straight wing (with Hand-GAL4)	Lethality (%)
Control (n=228)	115	113	1.7
UAS-Myc-Nedd4 (n=168)	90	78	13
UAS-Myc-Nedd4 (C/A) (n=211)	113	98	13
UAS-Nedd4-RNAi (n=159)	82	77	6.1

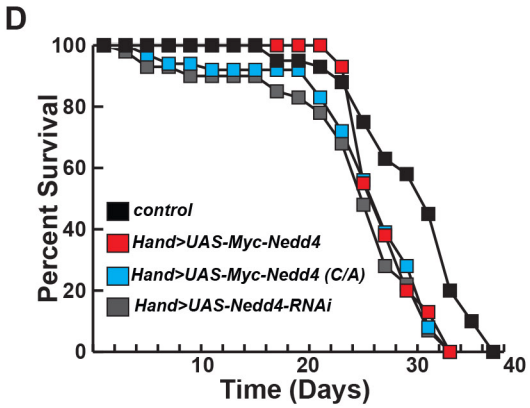

Fig. S4 Misexpression of dNedd4 Produces Abnormal Numbers of Cardioblasts and Mildly Decreases Fitness and Lifespan. (A–B) First-instar larvae marked by 20X magnification of first-instar larvae with genotypes as noted at bottom right. Anterior is to the left. (A'–B') 20X magnification of the area heighted by the yellow box noted in (A–B), with ostial cells outlined in dashed lines and cardioblasts marked by white arrows. Normally, four cardioblasts exist between each set of four ostial cells (A), while in *twist>UAS-Myc-dNedd4(C/A)* mutant larvae, the localization and/or number of these cardioblasts is abnormal (n=6 per phenotype). (C) Rates of eclosion by genotype at 29°C to enhance the temperature-sensitive UAS-transgene expression, with misexpression of dNedd4 mildly increasing lethality. (D) Adult male flies maintained at 29°C in vials containing approximately 15 animals. 60 flies were assayed per genotype, with misexpression of dNedd4 modestly decreasing life span.